

AD \_\_\_\_\_

Award Number: W81XWH-04-1-0061

TITLE: Angiogenesis-Independent Neovascularization is a Major Contributor to Tumor Growth

PRINCIPAL INVESTIGATOR: Alan J. Schroit, Ph.D.  
Weixin Lu, M.D., Ph.D.

CONTRACTING ORGANIZATION: The University of Texas  
M. D. Anderson Cancer Center  
Houston, TX 77030

REPORT DATE: September 2005

TYPE OF REPORT: Final

PREPARED FOR: U.S. Army Medical Research and Materiel Command  
Fort Detrick, Maryland 21702-5012

DISTRIBUTION STATEMENT: Approved for Public Release;  
Distribution Unlimited

The views, opinions and/or findings contained in this report are those of the author(s) and should not be construed as an official Department of the Army position, policy or decision unless so designated by other documentation.

**20060503104**

# REPORT DOCUMENTATION PAGE

*Form Approved*  
OMB No. 0704-0188

Public reporting burden for this collection of information is estimated to average 1 hour per response, including the time for reviewing instructions, searching existing data sources, gathering and maintaining the data needed, and completing and reviewing this collection of information. Send comments regarding this burden estimate or any other aspect of this collection of information, including suggestions for reducing this burden to Department of Defense, Washington Headquarters Services, Directorate for Information Operations and Reports (0704-0188), 1215 Jefferson Davis Highway, Suite 1204, Arlington, VA 22202-4302. Respondents should be aware that notwithstanding any other provision of law, no person shall be subject to any penalty for failing to comply with a collection of information if it does not display a currently valid OMB control number. **PLEASE DO NOT RETURN YOUR FORM TO THE ABOVE ADDRESS.**

<b>1. REPORT DATE</b> 01-09-2005			<b>2. REPORT TYPE</b> Final		<b>3. DATES COVERED</b> 15 Feb 2004 – 15 Aug 2005	
<b>4. TITLE AND SUBTITLE</b> Angiogenesis-Independent Neovascularization is a Major Contributor to Tumor Growth					<b>5a. CONTRACT NUMBER</b>	
					<b>5b. GRANT NUMBER</b> W81XWH-04-1-0061	
					<b>5c. PROGRAM ELEMENT NUMBER</b>	
<b>6. AUTHOR(S)</b> Alan J. Schroit,, Ph.D. Weixin Lu, M.D., Ph.D.					<b>5d. PROJECT NUMBER</b>	
					<b>5e. TASK NUMBER</b>	
					<b>5f. WORK UNIT NUMBER</b>	
<b>7. PERFORMING ORGANIZATION NAME(S) AND ADDRESS(ES)</b>  The University of Texas M. D. Anderson Cancer Center Houston, TX 77030					<b>8. PERFORMING ORGANIZATION REPORT NUMBER</b>	
<b>9. SPONSORING / MONITORING AGENCY NAME(S) AND ADDRESS(ES)</b> U.S. Army Medical Research and Materiel Command Fort Detrick, Maryland 21702-5012					<b>10. SPONSOR/MONITOR'S ACRONYM(S)</b>	
					<b>11. SPONSOR/MONITOR'S REPORT NUMBER(S)</b>	
<b>12. DISTRIBUTION / AVAILABILITY STATEMENT</b> Approved for Public Release; Distribution Unlimited						
<b>13. SUPPLEMENTARY NOTES</b>						
<b>14. ABSTRACT</b> Tumors must manipulate the host vasculature to provide a blood supply adequate for their proliferation. Although tumors may arise as avascular masses, there is increasing evidence that some tumors begin to proliferate by coopting the host vasculature. By analyzing cell proliferation kinetics of endothelial cells (EC) and PC3 prostate cancer cells, we provide evidence that EC proliferation could not account for rapid tumor growth. Although PC3mm2 expressing green fluorescent protein (GFP) failed to grow in the ears, in an orthotopic GFP – expressing melanoma model we demonstrated that the tumor vasculature was generated from a preexisting red cell-deficient vascular network that continuously remodeled to accommodate the requirements of the expanding tumor mass. Topical application of vascular endothelial growth factor (VEGF) to vascular beds generated immediate and robust vascular transitions that were morphologically similar to tumor-induced vascular transitions. N $\phi$ -nitro-L-arginine, a nitric oxide inhibitor that prevented VEGF-mediated vascular remodeling and vasodilatation, significantly inhibited prostate tumor growth without reducing EC proliferation. These findings suggest that prostate tumor-induced remodeling of red cell-deficient vessels, and not angiogenic sprouting, contributes to tumor vascularization and concomitant proliferation.						
<b>15. SUBJECT TERMS</b> prostate cancer, angiogenesis, tumor vascularization						
<b>16. SECURITY CLASSIFICATION OF:</b>			<b>17. LIMITATION OF ABSTRACT</b>	<b>18. NUMBER OF PAGES</b>	<b>19a. NAME OF RESPONSIBLE PERSON</b> USAMRMC	
<b>a. REPORT</b> U	<b>b. ABSTRACT</b> U	<b>c. THIS PAGE</b> U			<b>19b. TELEPHONE NUMBER</b> (include area code)	
			UU	16		

## Table of Contents

<b>Cover.....</b>	<b>1</b>
<b>SF 298.....</b>	<b>2</b>
<b>Introduction.....</b>	<b>4</b>
<b>Body.....</b>	<b>5</b>
<b>Key Research Accomplishments.....</b>	<b>9</b>
<b>Reportable Outcomes.....</b>	<b>9</b>
<b>Conclusions.....</b>	<b>9</b>
<b>References.....</b>	<b>9</b>
<b>Appendices.....</b>	<b>11</b>

## **Angiogenesis-independent "neovascularization" is a major contributor to tumor growth**

**Background:** The prevailing concept that tumor growth is dependent on angiogenesis, the formation of new blood vessels by sprouting from preexisting vessels, has led to intensive development of new antitumor therapies directed towards abrogating angiogenesis (1, 2). Although angiogenesis inhibitors have been in clinical trials for more than a decade, few have yielded clinical results predicted from preclinical animal trials despite the fact that many of these agents exhibit robust inhibitory effects on endothelial cell (EC) proliferation and migration *in vitro* (3). While these observations may seem to be incompatible, it is important to consider that despite the large body of evidence suggesting that angiogenesis is important for tumor development and by inference a target for cancer therapy (4), there is no unequivocal data demonstrating that angiogenesis is indeed a critical factor for tumor growth and metastasis. Thus, while angiogenesis is paramount to acute physiological processes such as development, pregnancy and wound healing, one must question whether it is equally crucial to the growth of human tumors.

Since antiangiogenic therapy has been intensively investigated in prostate cancer (5), understanding the precise mechanisms by which prostate cancer becomes vascularized is of utmost importance. We have developed and characterized a double-staining protocol that quantifies the number of proliferating EC in tumor tissue (the CD31/BrdU immunohistochemical double staining technique). We have also developed a novel real-time *in vivo* imaging system that allows us to survey, map, and characterize developing tumor-vasculature symbiosis in real time. Using this system we have investigated the contribution of true angiogenesis (new blood vessel growth) and blood vessel remodeling to prostate tumor growth.

**Specific Aims and Objective:** The objective of this proposal was to determine the mechanism primarily responsible for neovascularization of orthotopically and ectopically implanted human prostate carcinomas.

- 1) To determine the proliferation kinetics of tumor cells and EC in different areas within and surrounding the tumor at different stages of development.
- 2) To determine the role of preexisting host vasculature in prostate cancer vascularization.

**General methodological approach:** A new technique of double staining of CD31 antigen (for EC) and BrdU (for proliferating cells) on frozen sections was used to evaluate the relationship between the proliferation of EC and tumor cells. Real time observation of tumor growth of green fluorescent protein expressing PC3M cells *in vivo*, in combination with newly developed vascular surveying and mapping techniques were planned in order to reveal the dynamics and architecture of the tumor vasculature.

**Specific Study Design:** PC3M human prostate cancer cells were implanted ectopically into the subcutis or orthotopically into the prostate of nude mice. Tumors were harvested at various time points after inoculation. These cells were labeled with BrdU by injection 2 hrs prior to tumor harvest. Frozen sections were prepared and immunohistochemical double staining with antibodies against CD31 and BrdU was performed. The vascular morphology, EC labeling index, and tumor cell labeling index was analyzed in different zones within the tumor. To monitor

tumor vascularization in real-time, PC3M human prostate cancer cells were transfected with the green fluorescent protein (GFP) gene to express GFP. These cells were implanted ectopically into the subcutis. As described below, we encountered an unanticipated problem in that while the GFP transfected cells grew well *in vitro*, developing tumors spontaneously regressed when implanted the ear. Instead of abandoning this specific aim, we elected to complete these studies using GFP-transfected melanoma cells as a surrogate model. The rationale behind the design of these experiments and theoretical considerations of fluorescent quenching techniques appear in the Cancer Research publication in the appendix.

**Results:** To determine the contribution of EC proliferation to tumor growth, we implanted PC3mm2 human prostate cancer cells ( $2 \times 10^5$ ) into the prostates of nude mice. Tumor and adjacent tissue was collected at days 1, 2, 3, 5, 7, 14, 21 and 28. Frozen sections were prepared and the tissue was stained for CD31 (an EC label) and BrdU (a proliferating cell label). Table 1 shows that the fraction of BrdU-labeled EC in the center of small tumors decreased as tumor size increased. In larger tumors, BrdU-labeled EC were usually found within 1 mm of the tumor periphery. Regardless of tumor size, however, about 1/3 of tumor cells at the tumor margin were BrdU-positive. This suggests that tumor expansion was largely a result of these proliferating cells. The observations that virtually all EC within the core of large tumors did not divide, together with the disproportionate growth rates of EC and tumor cells suggest that EC proliferation was not responsible for tumor growth. Consistent with results found in other studies (6-8), there was no correlation between the labeling indices of EC and tumor cells ( $r^2=0.03$ ,  $P=0.22$ ) (Fig. 1).

**Table 1 Kinetics of BrdU labeling of endothelial and tumor cells in tumor development**

	Endothelial Cells				Tumor Cells	
	In Tumor		Normal Tissue Distant to Tumor Margin		Center	Periphery
	Center	Periphery	< 1mm	≥ 1mm		
Day 1		0%±0%	0%±0%	0%±0%		12%±4%
Day 2		2%±1%	0%±0%	0%±0%		27%±5%
Day 3		3%±1%	0%±0%	0%±0%		32%±3%
Day 5	3%±1%	3%±1%	0%±0%	0%±0%	16%±2%	32%±3%
Day 7	1%±1%	3%±1%	3%±1%	0%±0%	13%±2%	32%±2%
Day 14	0%±1%	3%±2%	3%±1%	0%±0%	9%±3%	30%±2%
Day 21	0%±0%	3%±2%	3%±1%	0%±0%	1%±1%	30%±2%
Day 28	0%±0%	3%±2%	3%±1%	0%±0%	1%±1%	29%±2%

PC3mm2 cells were injected into the prostates of nude mice. Tumors with their adjacent tissues were collected 2 hrs later after i.v. injection of 1 mg of BrdU at days 1, 2, 3, 5, 7, 14, 21 and 28 and prepared for CD31 and BrdU double staining. Periphery: ≤ 1 mm from tumor margin. Data are mean ±SD, the ratio of BrdU positive/total endothelial or tumor cells in each sample determined from measurement of 5 to 10 random 0.159 mm<sup>2</sup> fields at ×100 magnification.

Since exhaustive histological examination of tumor tissue failed to identify significant proliferating EC and tumor growth patterns characteristic of vessel co-option (9), other mechanisms likely contributed to tumor growth. To address this issue, we used fluorescence microscopy to enhance our ability to visualize and map small blood vessels in normal tissue and during tumor growth. Nude mice were injected *iv* with fluorescein (FITC)-labeled human serum albumin (FITC-HSA).

Fluorescence microscopy of ears revealed the presence of a large number of small fluorescent vessels that were not visible under bright-field. Conversely, bright-field illumination revealed patent, red blood cell-filled,

vessels that were not visible under fluorescent illumination due to inner filter effects of hemoglobin. After mapping the preexisting vascular network in the ears (Figs. 2A and B), we injected GFP-expressing K1735M2 melanoma cells into the subcutis of the mapped area and monitored tumor growth and vascularization daily<sup>1</sup>.

Figure 2 shows that blood vessels in the vicinity of the injection site became dilated within 1 day but returned to normal size within 48 hrs (attributed to a moderate inflammatory reaction at the site of injection). From day 5, however, a second vascular response resulted in the appearance of "new" blood vessels. These vessels seemed to sprout from the pre-existing large feeder vessel (Fig. 2A versus Fig. 2C). From day 7, the vessels became more dilated and tortuous and appeared to separate from each other at the tumor core (Fig. 2D-F). By day 13, some of the vessels became less visible and appeared to be engulfed or compressed by the outgrowing tumor (Fig. 2E). As the tumor expanded, it appeared to carry the peripheral vasculature with it by stretching and pushing the vessels ahead of its leading edge (Fig. 2E and F). This process led to an increase in the number of blood vessels at the tumor periphery and resulted in a high density of interweaving vessels at the tumor margin. It seems therefore that the continuous proliferation of the tumor dramatically changed the topography of its blood vessels. As the tumor grew, additional patent blood vessels appeared at the tumor margin. This included the sudden development of long vascular channels and blind-ended sprouts that pointed away from the tumor. Importantly, the pattern of these patent blood vessels closely followed the topography of

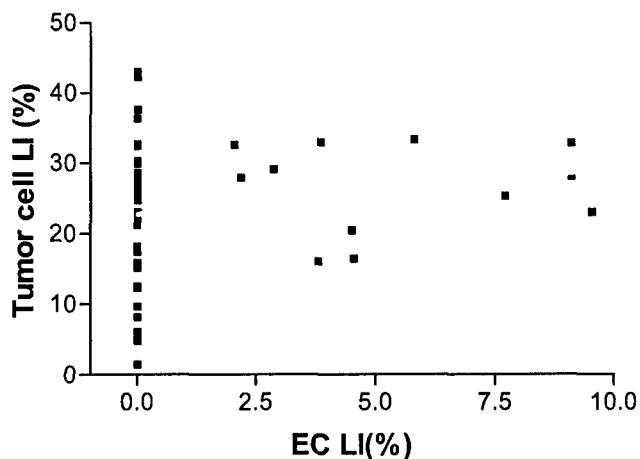


**Figure 1.** Correlation between fractions of BrdU labeled ECs and tumor cells. PC3mm2 cells were injected into prostate of nude mice, harvested on day 28 two hours later after intraperitoneal injection of BrdU, and stained for CD31 and BrdU. Fractions of BrdU labeled EC's and tumor cells were calculated in each randomized field, analyzed and plotted. ( $r^2=0.031$ ,  $P=0.22$ ).

<sup>1</sup> It should be noted that PC3mm2 cells failed to establish tumors in the ear. In an effort to establish the effect of tumor growth on the resident vasculature, we screened several tumors that could propagate in the mouse ear. Based on tumor growth characteristics we elected to carry out these studies with melanoma cells as surrogate for prostate cancer cells.

the previously mapped latent vessels present in the normal tissue prior to inoculation of the tumor cells. This observation raises the possibility that “angiogenic sprouting” is actually a result of progressive latent to patent blood vessel transitions.

To demonstrate that angiogenesis-like vascular morphological change can be induced without EC proliferation, we conducted real-time imaging experiments of blood vessel hemodynamics in the mesentery vascular bed. Mice were anesthetized and the mesentery was draped on the specimen stage of a dissecting microscope. Areas of interest were treated topically by administering vascular endothelial growth factor (VEGF) solution on the site once every 3 min. Sequential images were captured for 1 hr. Within 30 min after treatment, blood vessels in the area began to dilate, elongate and meander into torturous tubes. “New” patent blood vessels also became visible (Fig. 3)

The data presented above raise the possibility that tumor growth can be sustained, at least in part, by specifically increasing the availability of patent

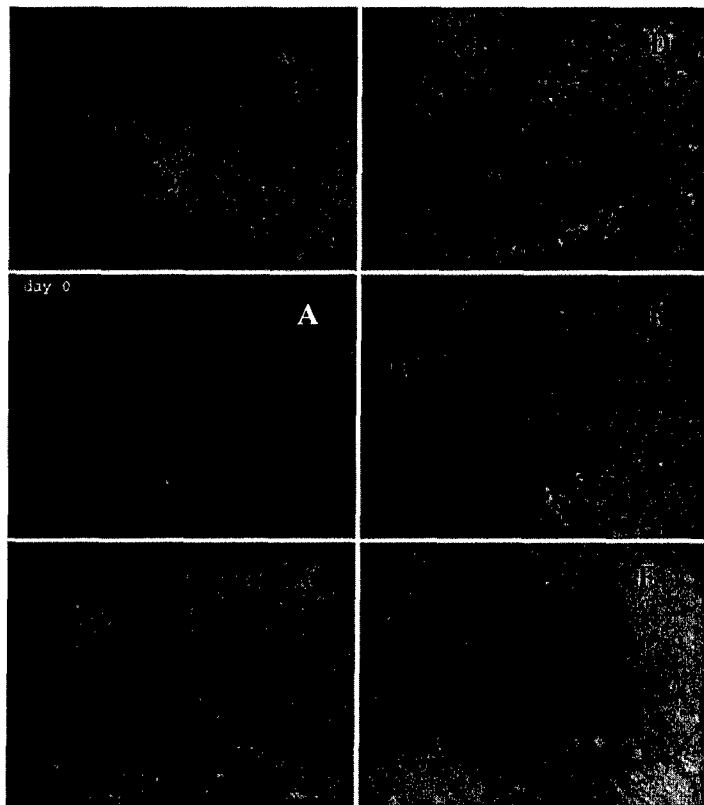


**Figure 2.** Patency of preexisting vasculature during K1735M2 melanoma growth in an ear of nude mouse. Nude mice were injected *i.v.* with FITC-HSA on day 0 to map the preexisting vascular network under bright field and fluorescence illumination.  $5 \times 10^4$  GFP-expressing K1735M2 melanoma cells in 5-10  $\mu$ L of saline were then injected into the subcutis of the ear. Tumor growth and vascularization were monitored by fluorescence (to determine tumor margins) and bright-field (patent vasculature) microscopy daily. Obvious latent to patent blood vessel transitions are numbered. Bar = 1mm.

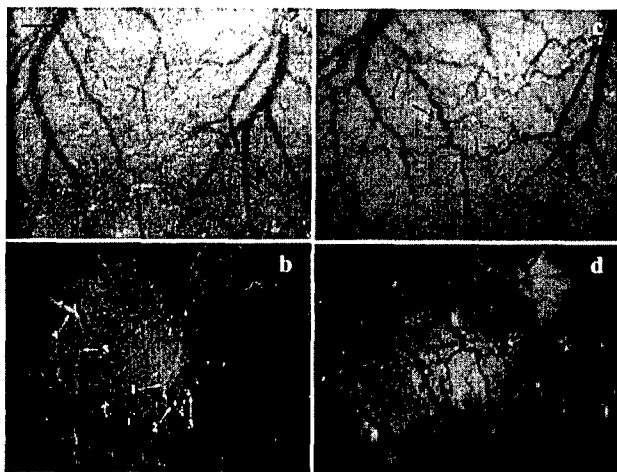


**Figure 3.** Blood vessel dilatation with VEGF. Mice were anesthetized and the mesentery was draped on the specimen stage of a dissecting microscope. Bright field and fluorescent images were collected before (a, b) and 1 hr after (c, d) treatment with VEGF. Note the increase in number of microvessels, vessel diameter and vessel tortuosity. Obvious latent to patent blood vessel transitions are numbered. Bar = 1mm.

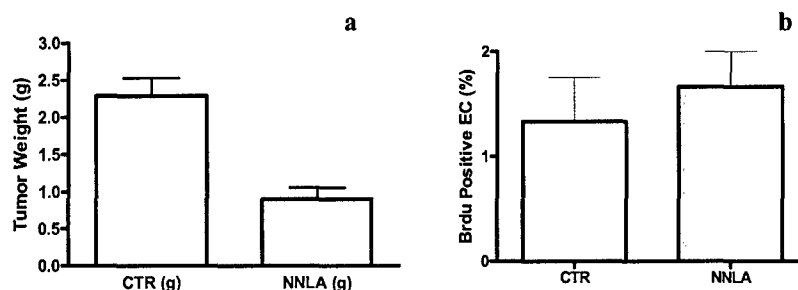


**Figure 4.** Comparison of prostate tumors weights (a) and BrdU-positive EC (b) after N-NLA treatment. PC3mm2 cells were inoculated into the prostate of nude mice. The mice were then randomized into group either receiving control drinking water or water containing 1 mg/ml of N-NLA. The mice were sacrificed 2 hours later after ip injection of BrdU when they became moribund, prostate tumors were harvested and weighed. Tumor tissues were double stained with BrdU and CD31 antibodies. BrdU positive endothelial cells were calculated.

blood vessels to tumors by a vasodilatation-dependent mechanism. If this is indeed the case, then one would expect that inhibition of blood vessel dilatation and concomitant latent to patent vascular transitions would significantly reduce tumor growth rate. To test this, tumor-bearing mice were treated with *N*-nitro-*L*-arginine (N-NLA), a potent nitric oxide inhibitor (10). Administration of N-NLA through the drinking water decreased PC3mm2 tumor growth by >50% ( $p < 0.05$ ) (Fig. 4A). To determine whether N-NLA-dependent decrease in tumor size was due to inhibition of EC proliferation, tumor thin sections from BrdU-injected control and N-NLA-treated mice were analyzed for BrdU-positive EC. Rigorous comparisons between groups revealed that while N-NLA decreased tumor size, no statistically significant difference was detected in the fraction of proliferating EC between groups (Fig. 4B).

It therefore seems that a proliferating tumor can modify preexisting capillary beds to facilitate the flow of red blood cells in a manner analogous to the “on-demand” blood supply in muscle that results in the opening of gated latent blood vessels (11). This likely proceeds through several phases that include relaxation of pre-capillary sphincters and dilatation of blood vessels by tumor-secreted factors (eg. VEGF/VPF) (12-15). EC then undergo a significant degree of stretch and hypertrophy (16) that results in further dilatation and lengthening of the vessels that accommodates the geographical requirements of the growing tumor without the need for angiogenesis. However, this mobilization and remodeling has limitations. If the capacity of the network is exceeded by the demands of the proliferating tumor, the tumor cells in an area where the blood vessels were fully mobilized will stop growing and eventually die. Unlike skin tumors that are amenable to real-time monitoring in live animals, blood vessel topography at other sites cannot be readily monitored by this technique. Nonetheless, assessment of EC proliferation in orthotopically-implanted PC3mm2 prostate cancer models revealed <3% of the EC labeled with BrdU, in sharp contrast with ~30% of the tumor cells labeled with BrdU (Table 1).

**Key Research Accomplishments:**

- 1) Cancer Research publication: Lu, W. and Schroit, A.J. (2005) Vascularization of melanoma by mobilization and remodeling of preexisting latent vessels to patency. *Cancer Res.* 65:913-918.
- 2) Pending publication: Vascularization of prostate tumors: Evidence for lack of angiogenesis.

**Reportable Outcome:** The results from the studies described here will form the basis for a new grant submission to the National Institutes of Health.

**Conclusions:** Based on these findings, we conclude that tumor vascularization depends on the interaction between invasive tumor and preexisting latent vascular beds. The tumor-dependent mobilization of these vessels to patency and their subsequent remodeling sustains tumor growth. The unabated radial intrusion of the tumor into normal tissue therefore results in a synergistic cascade of vessel activation and tumor expansion that leads to a larger tumor mass. This model predicts, therefore, that antiangiogenic therapy would be of limited efficacy and provides the basis for the development of alternative approaches to cancer therapy.

**Reference List**

1. Hanahan D, Weinberg RA. The hallmarks of cancer. *Cell* 2000;100:57-70
2. Kerbel R, Folkman J. Clinical translation of angiogenesis inhibitors. *Nature Rev. Cancer* 2002;2:727-739
3. Herbst RS, Hidalgo M, Pierson AS, Holden SN, Bergen M, Eckhardt SG. Angiogenesis inhibitors in clinical development for lung cancer. *Semin. Oncol.* 2002;29:66-77
4. Folkman J. What is the evidence that tumors are angiogenesis dependent? *J.Natl.Cancer Inst.* 1990;82:4-6
5. Nicholson B, Schaefer G, Theodorescu D. Angiogenesis in prostate cancer: biology and therapeutic opportunities. *Cancer Metastasis Rev.* 2001;20:297-319
6. Fox SB, Gatter KC, Bicknell R, Going JJ, Stanton P, Cooke TG, Harris AL. Relationship of endothelial cell proliferation to tumor vascularity in human breast cancer. *Cancer Res.* 1993;53:4161-4163
7. Denekamp J, Hobson B. Endothelial-cell proliferation in experimental tumours. *Bri. J. Cancer* 1982;46:711-720
8. Hobson B, Denekamp J. Endothelial proliferation in tumours and normal tissues: continuous labelling studies. *Bri. J. Cancer* 1984;49:405-413
9. Folkman J. Angiogenesis in cancer, vascular, rheumatoid and other disease. *Nature Med.* 1995;1:27-31

10. Cahlin C, Gelin J, Delbro D, Lonnroth C, Doi C, Lundholm K. Effect of cyclooxygenase and nitric oxide synthase inhibitors on tumor growth in mouse tumor models with and without cancer cachexia related to prostanoids. *Cancer Res.* 2000;60:1742-1749
11. Krogh, A. A Contribution to the physiology of the capillaries. Noble Lecture, December 11. [www.nobel.se/medicine/laureates/1920/krogh-lecture.html](http://www.nobel.se/medicine/laureates/1920/krogh-lecture.html) , 1-8. 1920.
12. Senger DR, Perruzzi CA, Feder J, Dvorak HF. A highly conserved vascular permeability factor secreted by a variety of human and rodent tumor cell lines. *Cancer Res.* 1986;46:5629-5632
13. Dvorak HF, Sioussat TM, Brown LF, Berse B, Nagy JA, Sotrel A, Manseau EJ, Van de WL, Senger DR. Distribution of vascular permeability factor (vascular endothelial growth factor) in tumors: concentration in tumor blood vessels. *J. Exp. Med.* 1991;174:1275-1278
14. Dvorak HF, Nagy JA, Feng D, Brown LF, Dvorak AM. Vascular permeability factor/vascular endothelial growth factor and the significance of microvascular hyperpermeability in angiogenesis. *Curr. Top. Microbiol. Immunol.* 1999;237:97-132
15. Dafni H, Landsman L, Schechter B, Kohen F, Neeman M. MRI and fluorescence microscopy of the acute vascular response to VEGF165: vasodilation, hyper-permeability and lymphatic uptake, followed by rapid inactivation of the growth factor. *NMR in Biomed.* 2002;15:120-131
16. Dvorak HF. Rous-Whipple Award Lecture. How tumors make bad blood vessels and stroma. *Amer. J. Pathol.* 2003;162:1747-1757

# Vascularization of Melanoma by Mobilization and Remodeling of Preexisting Latent Vessels to Patency

Weixin Lu and Alan Jay Schroit

Department of Cancer Biology, University of Texas M.D. Anderson Cancer Center, Houston, Texas

## Abstract

Tumors must manipulate the host vasculature to provide a blood supply adequate for their proliferation. Although tumors may arise as avascular masses, there is increasing evidence that some tumors begin to proliferate by first co-opting preexisting host blood vessels. By fluorescent vascular imaging, we provide evidence that the vasculature in orthotopically implanted melanoma arises from a preexisting red cell-deficient vascular network that remodels to patency to accommodate the requirements of the expanding tumor mass. Topical application of vascular endothelial growth factor to vascular beds generated immediate and robust vascular transitions that were morphologically similar to tumor-induced transitions. *N*<sup>o</sup>-nitro-L-arginine, a nitric oxide inhibitor, significantly inhibited the growth of a syngeneic K1735M2 melanoma by reducing blood supply to the tumor by a mechanism independent of endothelial cell proliferation. These findings suggest that tumor-induced remodeling of red cell-deficient vessels to patency contributes to tumor vascularization and growth. (Cancer Res 2005; 65(3): 913-8)

## Introduction

The growth and dissemination of tumors depends on the establishment of an adequate blood supply to provide nutrients sufficient for their proliferation. Although it is widely accepted that development of a neovasculature through various angiogenic mechanisms is critical for tumor development (1-3), there is increasing evidence that co-option of preexisting vascular beds by the proliferating tumor plays an important role in the early stages of tumor growth in highly vascularized tissues (4-6). Typically, these tumors expand along the capillaries to produce multiple diffuse lesions within the parenchyma (7).

In many tissues, a large fraction of the capillary beds remain closed to the flow of red cells for long periods due to contraction of precapillary sphincters. This typically occurs in muscle where exercise-induced hypoxia (decreased pO<sub>2</sub>) stimulates their relaxation and induces vessel dilation to provide a large reserve flow capacity and red cell flux that accommodates the increased oxygen demand of the working tissue (8). Because relaxation of precapillary sphincters and contractile tone of capillary pericytes is under the control of local metabolic factors (9-12), we hypothesized that tumor growth is partly dependent on a similar mechanism. Indeed, proliferating tumors produce factors that effect endothelial cell migration, proliferation, and vessel dilation (13-15).

Requests for reprints: Alan Jay Schroit, Department of Cancer Biology (173), University of Texas M.D. Anderson Cancer Center, 1515 Holcombe Boulevard, Houston, TX 77030. Phone: 713-792-8586; Fax: 713-792-8747; E-mail: aschroit@mdanderson.org.

©2005 American Association for Cancer Research.

To define the contribution of preexisting vasculature to tumor growth, we mapped resident patent (normal hematocrit) and latent (red cell-deficient) vessels in normal mouse skin by imaging fluorescein-conjugated, albumin-perfused blood vessels. The topography of the premapped vasculature was then monitored in live animals after inoculation of melanoma cells. In parallel, endothelial cell proliferation within the tumor was estimated by the proliferation-dependent incorporation of BrdUrd into CD31-positive endothelial cells. We show that normal skin has a substantial red cell-deficient vascular network that the tumor mobilizes to patency. Blocking this process with a nitric oxide inhibitor inhibited tumor growth.

## Materials and Methods

**Animals, Cells, and Reagents.** Specific pathogen-free female C3H/HeN and *nu/nu* mice were purchased from the National Cancer Institute-Frederick Cancer Research Facility (Frederick, MA). K1735M2 melanoma cells were derived from a spontaneous lung metastases produced from parental K1735 cells originally induced in C3H/HeN mice by UVB radiation (16). K1735M2 cells were transfected with pEGFP1 (Clontech Laboratories, Inc., Palo Alto, CA) using FuGene VI transfection reagents (Roche Molecular Biochemicals, Indianapolis, IN) according to the protocol of the manufacturer. Cells were harvested after 48 hours by trypsinization and subcultured at a ratio of 1:15 in G418-containing medium (800 µg/mL). Clones that expressed high-intensity green fluorescent protein were pooled and used for the *in vivo* studies. Fluorescein-conjugated albumin (FITC-SA) was prepared by incubating human serum albumin (12.5 mg/mL) with FITC (1 mg/mL) in 0.1 mol/L sodium carbonate (pH 9.0) for 8 hours at 4°C. Unreacted FITC was removed by dialysis or by column chromatography. Quench curves were generated by plotting the fluorescence intensity of FITC-SA solutions in the absence (*I*<sub>F1</sub>) and presence (*I*<sub>F2</sub>) of the indicated concentrations of red cells, where:

$$\% \text{Quench} = 100[(I_{F1} - I_{F2})/I_{F1}]$$

**Immunofluorescence.** To monitor endothelial cell proliferation within tumors, animals were injected with BrdUrd (1 mg) 2 hours before tumor harvest. Acetone-fixed frozen sections (5 µm) were sequentially incubated with rat anti-mouse CD31 (PharMingen, San Diego, CA) and Texas red-conjugated goat anti-rat antibodies (Jackson ImmunoResearch Laboratories, West Grove, PA). For BrdUrd staining, the thin sections were postfixed with paraformaldehyde (4%), permeabilized with 0.2% Triton X-100/2 N HCl, and stained with monoclonal BrdUrd antibody (Becton Dickinson Immunocytometry, San Jose, CA) followed by Alexa 488-conjugated goat anti-mouse IgG (Molecular Probes, Eugene, OR). Fluorescence microscopy was done with an epifluorescence microscope equipped with a mercury vapor lamp and appropriate narrow bandpass excitation and emission filters (Ludl Electronic Products, Hawthorne, NY).

**Intravital Microscopy.** Mice were anesthetized by metaflane inhalation for imaging and recording purposes. Metaflane inhalation did not affect blood vessel topography. Normal (pre-tumor) nude mouse ears were mapped with FITC-SA under both bright-field and fluorescent illumination.

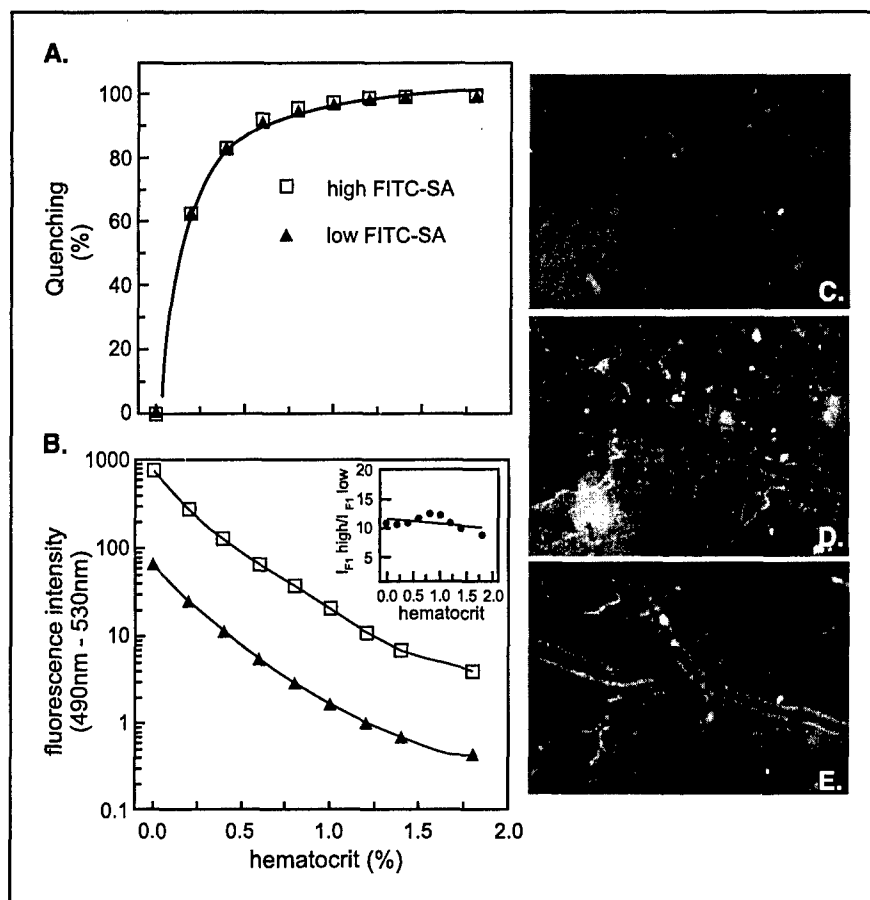


**Figure 1.** Quenching of FITC-albumin (FITC-SA) fluorescence by red cells. Aliquots of RBC (50% packed cells) were added to mouse plasma containing 50  $\mu$ g/mL ( $\square$ ) and 5  $\mu$ g/mL ( $\blacktriangle$ ) FITC-SA. Points, percentage of fluorescence quenched by increasing RBC (A) and actual relative fluorescent intensities (B). B, inset, fluorescence intensity ratios of high- and low-dose FITC-SA as a function of hematocrit. C and D, a mouse was injected in the tail vein with 50  $\mu$ L FITC-SA (0.1 mg/mL) and photographed under combined bright-field and fluorescence (C) or fluorescence illumination only (D). An additional 50  $\mu$ L aliquot of FITC-SA (1 mg/mL) was then injected (E). Note that some intensely fluorescent blood vessels (D) are also visible under combined fluorescent and bright-field illumination (C).

To accurately determine the location and topography of the inoculated tumor cells at the initial stage of growth, green fluorescent protein-expressing K1735 melanoma cells ( $5 \times 10^4$  cells in 5-10  $\mu$ L of saline) were injected into the subcutis of the right ear. Left ears were injected with saline alone and served as individual controls for each mouse. Tumor-dependent vascular alterations were imaged in live mice using a fluorescence stereo microscope (Leica model LZ12) equipped with narrow bandpass excitation and emission filters mounted in a selectable filter wheel (Ludl Electronic Products). Real-time images were directly captured with an Evolution MP camera (Media Cybernetics, Inc., Silver Spring, MA) or by frame capture from videotaped images. Image analyses were independently carried out in five mice. The images presented are typical and consistent with results obtained in every animal.

**Determination of Tumor Blood Volumes.** Tumor-bearing mice were injected i.v. with 0.1 mL of 40% packed syngeneic RBC labeled with  $^{51}\text{Cr}$  (1.0 mCi/mL packed red cells for 10 minutes at 37°C). After  $\sim$ 10 minutes, 5 to 10  $\mu$ L of tail vein blood were collected, the mice were killed, and tumors were removed. Radiation in the blood and tumors was quantified by scintillation counting. Tumor blood volume was determined from tumor-associated radiation per gram of tissue standardized from counts per minute per microliter of blood calculated from the tail vein sample.

**N-nitro-L-arginine Treatment, Tumor Growth, and Vascular Permeability (Miles) Assay.** N-nitro-L-arginine (N-NLA) was given to mice *ad libitum* through the drinking water (1 mg/mL) beginning on the day of tumor inoculation. The Miles assay (17) was done on N-NLA-treated or untreated mice. Briefly, mice were injected i.d. with vascular endothelial growth factor (VEGF; 50  $\mu$ L at 50 ng/mL). After 10 minutes, mice were injected i.v. with 0.2 mL of 0.5% Evans blue dye (Sigma, St. Louis, MO) in PBS. Dye release at the VEGF injection site was recorded 30 minutes later. Tumor growth was monitored in C3H/HeN mice injected s.c. with

$2 \times 10^5$  K1735M2 melanoma cells. The mice were randomized into groups of 10 mice each that received drinking water with and without N-NLA. Tumor size was estimated by measuring two perpendicular diameters with calipers every week. Tumor volumes were calculated by  $0.56 \times a \times b^2$ , where  $a$  and  $b$  are the long and short diameters, respectively.

**Statistical Analysis.** Data were expressed as mean  $\pm$  SD. ANOVA and Student's  $t$  test were used for data analysis.

## Results

### Differentiation of Latent and Patent Blood Vessels *In vivo*.

To address the potential role of latent vasculature in supporting the establishment and progression of tumors, a model system that differentiates between preexisting latent (closed) and patent (open) vessels in live animals was developed. The protocol takes advantage of the ability of red cells to quench fluorescein fluorescence through the inner filter effects of hemoglobin. The technique is based on observations that the extent of fluorescence quenching is dependent on hematocrit (percentage of packed red cell volume) and independent of fluorophore concentration (Fig. 1A). As plotted in Fig. 1B (inset), the relative fluorescence intensity at any given hematocrit is a constant that is independent of fluorophore concentration. In principle, therefore, concentrations of fluorophores can be selected such that latent (red cell-deficient) vessels fluoresce and patent (red cell-rich) vessels do not. Thus, fluorescence detection of blood vessels with increasing red cell content requires increasing concentration of fluorophore (Fig. 1B). To test this, anesthetized mice were injected with

increasing concentrations of FITC-SA. Fluorescence microscopy of ears in live nude mice injected with low concentrations of FITC-SA revealed the presence of a large number of small fluorescent vessels (Fig. 1D) that were mostly not visible under bright-field illumination (Fig. 1C). Conversely, red blood vessels visible under bright field were mostly nonfluorescent and appeared as negative images. Figure 1E shows that injection of an additional aliquot of fluorophore breached the quenching threshold of the large red cell-filled vessels and became fluorescent. Thus, the fluorescent-visible vessels at low concentrations of FITC-SA contained very low concentrations of red cells. Taken together, these data indicate that normal tissue contains a network of red cell-deficient blood vessels that can be differentiated from patent vessels in live animals by carefully controlling the concentration of fluorophore *in vivo*.

**Tumor-Induced Mobilization and Remodeling of Red Cell-Deficient Vasculature.** After mapping the preexisting vascular network in the ears of *nu/nu* mice (Fig. 2A and B), green fluorescent protein-expressing K1735M2 melanoma cells were injected into the subcutis of the mapped area. Tumor growth and vascular patency were assessed daily by monitoring green fluorescent protein expression and red blood vessels, respectively. Vessels near the injection site became dilated within 1 day but returned to normal size within 48 hours (attributed to a moderate inflammatory reaction at the site of injection). From day 5, however, a second vascular response resulted in the appearance of previously invisible red blood vessels that duplicated the pattern of

the mapped preexisting fluorescent vascular bed. The origin of these vessels was traced to the preexisting large red feeder vessel (Fig. 2A versus Fig. 2C). From day 7, the vessels became more dilated and tortuous and appeared to separate from each other at the tumor core (Fig. 2D-F). By day 13, some of the vessels became less visible and appeared to be engulfed or compressed by the outgrowing tumor (Fig. 2E). As the tumor expanded more, it appeared to carry the peripheral vasculature with it by stretching and pushing the vessels ahead of its leading edge (Fig. 2E and F). This process led to an increase in the density of interweaving vessels at the tumor margin. It seems, therefore, that the continuous proliferation of the tumor dramatically changed both the topography and the patency of the preexisting latent vascular network. Importantly, daily monitoring of the dynamic changes in the pattern of tumor blood vessels revealed that the new bright-field visible red blood vessels could be traced back to the corresponding previously mapped latent vessels present in the tissue before inoculation of the tumor cells. Control ears (left) of the same mice injected with identical volumes of inoculate without tumor cells showed some vascular dilation at the site of injection that resolved within 48 hours. This observation suggests that tumors can acquire a blood supply by co-opting latent vascular beds that are progressively mobilized to patency.

**VEGF-Induced Angiogenesis-Like Vascular Remodeling.** The data presented above suggest that tumor-dependent alterations in blood vessel function result in the influx of red cells that contributes

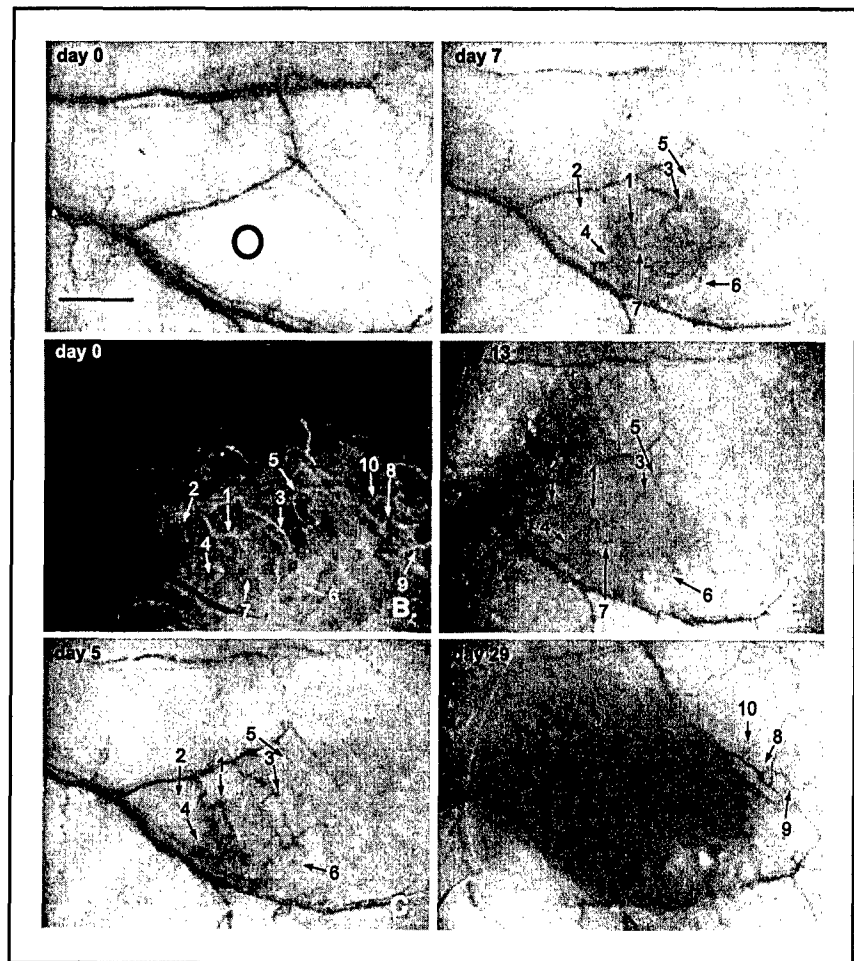


**Figure 2.** Patency of preexisting vasculature during K1735M2 melanoma growth in an ear of nude mouse. Nude mice were injected i.v. with FITC-SA on day 0 to map the vasculature under bright-field and fluorescence illumination. Green fluorescent protein-expressing K1735M2 melanoma cells ( $5 \times 10^4$ ) in 5 to 10  $\mu$ L of saline were then injected into the subcutis of the ear. Tumor growth and vascularization were monitored by fluorescence (to determine tumor margins) and bright-field (patent vasculature) microscopy daily. A, circle, inoculation site. Obvious latent to patent blood vessel transitions are numbered. Bar, 1 mm.

to tumor growth. Because VEGF is an important tumor angiogenic factor that also induces persistent vasodilation and increased vasopermeability (13–15), we tested whether the vascular alterations observed in the tumor system could be reproduced with VEGF alone. VEGF-induced vascular alterations were monitored in real time by imaging blood vessel hemodynamics in mesenteric vascular beds. Mice were anesthetized, and the mesentery was draped on the specimen stage of a dissecting microscope. Areas of interest were treated by topically applying VEGF. Sequential bright-field and fluorescent images captured for 1 hour showed that the blood vessels began to dilate, elongate, and form torturous tubes within 10 minutes after the addition of VEGF. Examination of time-matched, bright-field and fluorescent images revealed new red blood vessels (Fig. 3C) that were visible only under fluorescence illumination before the addition of VEGF (Fig 3A versus Fig. 3B) and, on reaching patency, could be seen under bright-field and fluorescent illumination as red-positive (Fig. 3C) and fluorescent-negative (Fig. 3D) images, respectively. The topography of the blood vessels was unchanged on treatment with diluent (0.1% bovine serum albumin in saline) alone.

**Inhibition of Tumor Growth with N-NLA.** The data presented above raise the possibility that tumor growth can be sustained, at least in part, by specifically increasing the availability of patent blood vessels to tumors by a vasodilation-dependent mechanism. If this is indeed the case, then one would expect that inhibition of blood vessel dilation and concomitant latent to patent vascular transitions would significantly reduce tumor growth rate. To test this, tumor-bearing mice were treated with N-NLA, a potent nitric oxide inhibitor (18). Administration of N-NLA through the drinking water decreased K1735M2 tumor growth by ~90% ( $P < 0.01$ ; Fig. 4A) and reduced tumor blood volume by 28% ( $9.15 \pm 4.50 \mu\text{L/g}$  tumor for control versus  $6.60 \pm 1.26 \mu\text{L/g}$  tumor for N-NLA;  $P < 0.05$ ). Treatment with N-NLA also inhibited VEGF-induced vascular

permeability (Fig. 4B). To determine whether N-NLA-dependent decrease in tumor size and blood volume was due to inhibition of endothelial cell proliferation, tumor thin sections from BrdUrd-injected control and N-NLA-treated mice were analyzed for BrdUrd-positive endothelial cells. Rigorous comparisons among groups revealed that whereas N-NLA decreased tumor size, a small but significant increase in the fraction of BrdUrd-labeled, CD31-positive endothelial cells in the tumor periphery was observed ( $2.2 \pm 0.4\%$  versus  $5.4 \pm 0.6\%$  for control and N-NLA-treated animals, respectively;  $P < 0.05$ ). This increase might reflect compensatory endothelial cell proliferation-mediated angiogenesis in the presence of N-NLA-dependent inhibition of blood vessel dilation.

#### Endothelial Cell Proliferation during Tumor Development.

Because inhibition of tumor growth by N-NLA appeared to occur through an endothelial cell proliferation-independent pathway, we further analyzed the potential contribution of proliferating endothelial cells to tumor growth. K1735M2 mouse melanoma cells ( $2 \times 10^5$ ) were implanted into the subcutis of syngeneic C3H/HeN mice, and tumor together with adjacent tissue was collected at days 1, 2, 3, 5, 7, 13, and 23. Frozen sections were prepared, and the tissue was stained for CD31 (an endothelial cell label) and BrdUrd (a proliferating cell label). Table 1 shows that the fraction of BrdUrd-labeled endothelial cell in the center of small tumors (<7 days; <2 mm diameter) decreased as tumor size increased. In larger tumors (>13 days; >5 mm diameter), BrdUrd-labeled endothelial cell were usually found only within 1 mm of the tumor periphery. In contrast, regardless of tumor size, about one third of tumor cells at the tumor margin were BrdUrd positive.

#### Discussion

It is widely accepted that small tumors remain dormant in the absence of angiogenesis and that tumor growth can be suppressed by inhibiting angiogenesis (19). Although development

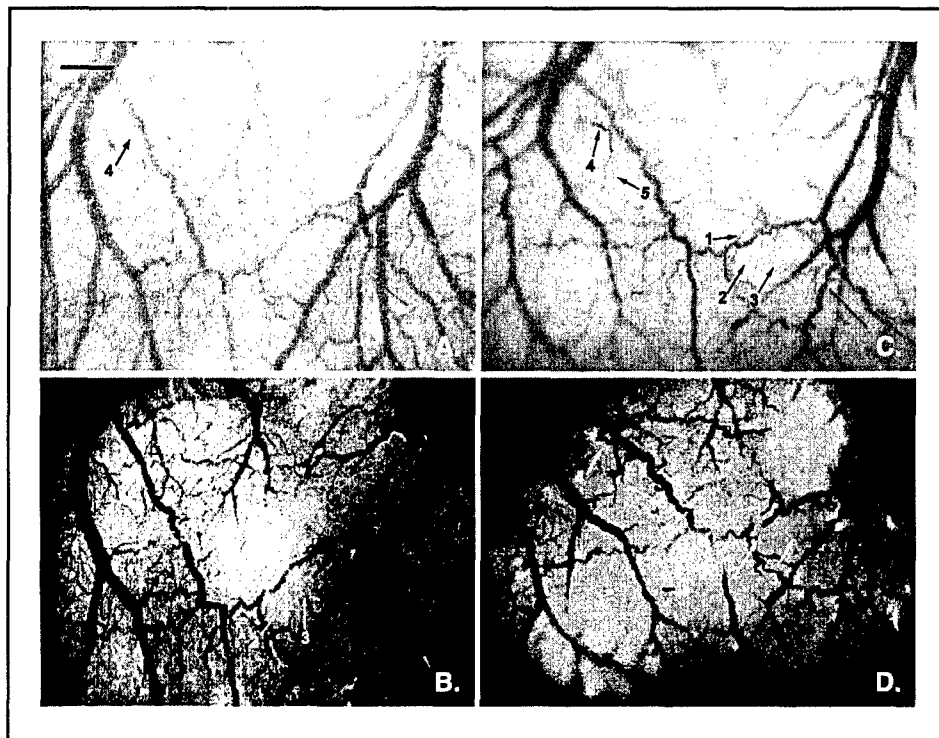
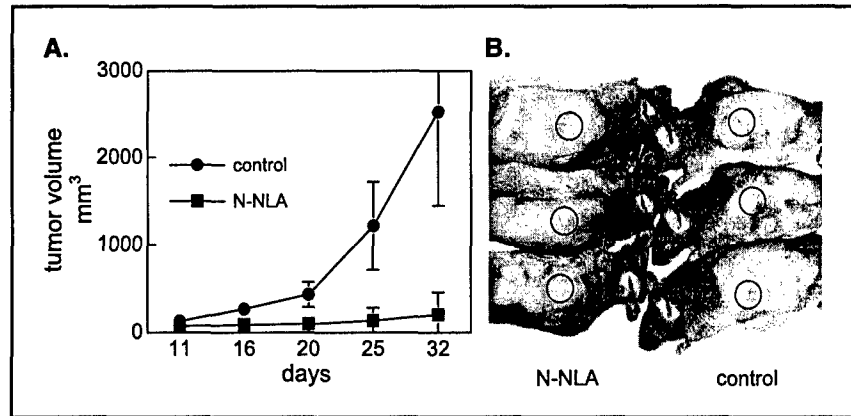


**Figure 3.** Blood vessel dilation with VEGF. C3H/HeN mice were anesthetized, and the mesentery was draped on the specimen stage of a dissecting microscope. Bright-field and fluorescent images were collected before (A and B) and 1 hour after (C and D) treatment with VEGF. Note the increase in number of microvessels, vessel diameter, and vessel tortuosity. Obvious latent to patent blood vessel transitions are numbered. For example, in control tissue, the vessel at arrow 4 is not visible in A but is green in B. This vessel became visible under bright field after the addition of VEGF (C) and appeared as a negative image (D). Bar, 1 mm.

**Figure 4.** Inhibition of tumor growth and vascular permeability in N-NLA-treated mice. **A**, C3H/HeN mice were inoculated in the flank s.c. with K1735M2 melanoma cells and randomized into control and N-NLA-treated groups. Tumor growth was then monitored. **B**, at the end of the experiment, N-NLA-treated and control animals were injected i.d. with VEGF, and vascular permeability is described in Materials and Methods. *Circles*, injection sites.



of angiogenesis inhibitors focuses on inhibition of tumor-induced endothelial cell proliferation that leads to angiogenic sprouting, evidence that tumor growth can be sustained by endothelial cell proliferation-independent mechanisms of vascular expansion is accumulating (6, 20). Because proangiogenic factors, like VEGF (6) and basic fibroblast growth factor (10), are also potent blood vessel dilators, it is possible that some antiangiogenic therapies might be affected by mechanisms other than abrogation of endothelial cell proliferation. Because the tumor blood vessels are present in the dermis before inoculation of tumor, the data presented here provide evidence for a mechanism in which preexisting plasma-perfused but red cell-poor vessels are co-opted by tumor that topographically and functionally remodels it to patency in a manner that is morphologically indistinguishable from endothelial cells proliferation-dependent angiogenesis. The significant divergence in the fraction of proliferating endothelial cells and proliferating tumor observed in all stages of tumor growth (Table 1) further suggests that endothelial cell proliferation-mediated vascular expansion alone cannot accommodate the vascular demands imposed by the proliferating tumor. In principle, tumor growth can be accommodated in the absence of significant proliferation-dependent angiogenesis through VEGF-mediated endothelial cell mobilization and remodeling that

characteristically lead to increases in cell surface area and vascular dilation and lengthening (up to >3 times the original size) without membrane synthesis (21). Nitric oxide is the primary vasodilatory mediator (22, 23), and competitive inhibition of nitric oxide synthase with L-arginine analogues results in decreased tumor growth rates (18) because of decreased tumor blood flow (23, 24).

Taken together, these data support a model in which a proliferating tumor modifies preexisting capillary beds to facilitate the flow of RBC in a manner analogous to the "on-demand" opening of gated latent blood vessels in muscle. This likely proceeds through several steps that include relaxation of precapillary sphincters and dilation of blood vessels by tumor-secreted factors (e.g., VEGF/VPF; refs. 13, 25-27). Unlike the concept that tumor growth is dependent on ingrowth of a new vasculature, the data presented here show orthotopically implanted melanoma grow by co-opting and mobilizing a latent vasculature that is morphologically similar to angiogenic sprouting. This model predicts, therefore, that tumor expansion depends on the unabated radial intrusion of tumor into preexisting latent vascular beds that topographically and functionally remodel to accommodate the requirements of the enlarging tumor mass.

**Table 1.** BrdUrd labeling of endothelial cells and tumor cells during tumor development

Time post-implantation (d)	% of Endothelial cells				% of Tumor cells	
	In tumor		In normal tissue (distance from tumor margin)		Center	Periphery
	Center	Periphery	<1 mm	1 mm		
1		0 ± 1	0 ± 0	0		16 ± 5
2		5 ± 2	1 ± 2	0		27 ± 5
3		3 ± 2	0 ± 0	0		33 ± 4
5		5 ± 3	0 ± 0	0		36 ± 12
7	2 ± 4	4 ± 3	3 ± 1	0	14 ± 4	35 ± 11
13	1 ± 1	4 ± 4	4 ± 2	0	12 ± 5	32 ± 4
23	0 ± 0	3 ± 3	3 ± 1	0	1 ± 1	30 ± 3

NOTE: K1735M2 cells ( $2 \times 10^5$ ) were injected s.c. into the flank of C3H/HeN mice. The injection was marked, and tumors together with adjacent tissue were collected 2 hours after i.v. injection of BrdUrd (1 mg) at the indicated days and stained for CD31 and BrdUrd. Periphery: <1 mm from the tumor margin. Mean ± SD of the ratio of BrdUrd positive to total number of endothelial cells and tumor cells in each sample determined from measurements in 5 to 10 random 0.159-mm<sup>2</sup> fields. Because palpable tumors were not present until day 5, tissue was collected from the marked injection site.

## Acknowledgments

Received 8/9/2004; revised 11/3/2004; accepted 11/18/2004.

Grant support: NIH grant CA47845, Department of Defense grant PC030875, and John Q. Gaines Foundation.

The costs of publication of this article were defrayed in part by the payment of page charges. This article must therefore be hereby marked advertisement in accordance with 18 U.S.C. Section 1734 solely to indicate this fact.

We thank Drs. Lee Ellis, Mien-Chie Hung, Isaiah J. Fidler, and Robert Langley for helpful discussions and advice.

## References

- Carmeliet P, Jain RK. Angiogenesis in cancer and other diseases. *Nature* 2000;407:249-57.
- Folkman J. Role of angiogenesis in tumor growth and metastasis. *Semin Oncol* 2002;29:15-18.
- Bergers G, Benjamin LE. Tumorigenesis and the angiogenic switch. *Nat Rev Cancer* 2003;3:401-10.
- Holash J, Wiegand SJ, Yancopoulos GD. New model of tumor angiogenesis: dynamic balance between vessel regression and growth mediated by angiopoietins and VEGF. *Oncogene* 1999;18:5356-62.
- Holash J, Maisonpierre PC, Compton D, et al. Vessel cooption, regression, and growth in tumors mediated by angiopoietins and VEGF. *Science* 1999;284:1994-8.
- Kusters B, Leenders WP, Wesseling P, et al. Vascular endothelial growth factor-A(165) induces progression of melanoma brain metastases without induction of sprouting angiogenesis. *Cancer Res* 2002;62:341-5.
- Fidler IJ, Yano S, Zhang RD, Fujimaki T, Bucana CD. The seed and soil hypothesis: vascularisation and brain metastases. *Lancet Oncol* 2002;3:53-7.
- Krogh A. A Contribution to the physiology of the capillaries. Noble Lecture. 1920 [cited 1920 Dec 11];1-8. Available from: <http://www.nobel.se/medicine/laureates/1920/krogh-lecture.html>.
- Granger HJ, Goodman AH, Cook BH. Metabolic models of microcirculatory regulation. *Fed Proc* 1975;34:2025-30.
- Wu HM, Yuan Y, McCarthy M, Granger HJ. Acidic and basic FGFs dilate arterioles of skeletal muscle through a NO-dependent mechanism. *Am J Physiol* 1996; 271:H1087-93.
- Anderson DR, Davis EB. Glaucoma, capillaries and pericytes. Preliminary evidence that carbon dioxide relaxes pericyte contractile tone. *Ophthalmology* 1996; 210:280-4.
- Pallone TL, Zhang Z, Rhinehart K. Physiology of the renal medullary microcirculation. *Am J Physiol* 2003;284:F253-66.
- Dvorak HF, Nagy JA, Feng D, Brown LF, Dvorak AM. Vascular permeability factor/vascular endothelial growth factor and the significance of microvascular hyperpermeability in angiogenesis. *Curr Top Microbiol Immunol* 1999;237:97-132.
- Pettersson A, Nagy JA, Brown LF, et al. Heterogeneity of the angiogenic response induced in different normal adult tissues by vascular permeability factor/vascular endothelial growth factor. *Lab Invest* 2000;80:99-115.
- Nagy JA, Vasile E, Feng D, et al. Vascular permeability factor/vascular endothelial growth factor induces lymphangiogenesis as well as angiogenesis. *J Exp Med* 2002;196:1497-506.
- Talmadge JE, Fidler IJ. Enhanced metastatic potential of tumor cells harvested from spontaneous metastases of heterogeneous murine tumors. *J Natl Cancer Inst* 1982;69:975-80.
- Dvorak HF, Orenstein NS, Carvalho AC, et al. Induction of a fibrin-gel investment: an early event in line 10 hepatocarcinoma growth mediated by tumor-secreted products. *J Immunol* 1979;122:166-74.
- Cahlin C, Gelin J, Delbro D, Lonnroth C, Doi C, Lundholm K. Effect of cyclooxygenase and nitric oxide synthase inhibitors on tumor growth in mouse tumor models with and without cancer cachexia related to prostanoids. *Cancer Res* 2000; 60:1742-9.
- Udagawa T, Fernandez A, Achilles EG, Folkman J, D'Amato RJ. Persistence of microscopic human cancers in mice: alterations in the angiogenic balance accompanies loss of tumor dormancy. *FASEB J* 2002; 16:1361-70.
- Ribatti D, Vacca A, Dammacco F. New non-angiogenesis dependent pathways for tumour growth. *Eur J Cancer* 2003;39:1835-41.
- Dvorak HF. Rous-Whipple Award Lecture. How tumors make bad blood vessels and stroma. *Am J Pathol* 2003;162:1747-57.
- Tozer GM, Everett SA. Nitric oxide in tumour biology and cancer therapy. Part 1: physiological aspects. *Clin Oncol (R Coll Radiol)* 1997;9:282-93.
- Tozer GM, Prise VE, Wilson J, et al. Mechanisms associated with tumor vascular shut-down induced by combretastatin A-4 phosphate: intravital microscopy and measurement of vascular permeability. *Cancer Res* 2001;61:6413-22.
- Andrade SP, Hart IR, Piper PJ. Inhibitors of nitric oxide synthase selectively reduce flow in tumor-associated neovasculature. *Br J Pharmacol* 1992;107: 1092-5.
- Senger DR, Perruzzi CA, Feder J, Dvorak HF. A highly conserved vascular permeability factor secreted by a variety of human and rodent tumor cell lines. *Cancer Res* 1986;46:5629-32.
- Dvorak HF, Sioussat TM, Brown LF, et al. Distribution of vascular permeability factor (vascular endothelial growth factor) in tumors: concentration in tumor blood vessels. *J Exp Med* 1991; 174:1275-8.
- Dafni H, Landsman L, Schechter B, Kohen F, Neeman M. MRI and fluorescence microscopy of the acute vascular response to VEGF165: vasodilation, hyper-permeability and lymphatic uptake, followed by rapid inactivation of the growth factor. *NMR Biomed* 2002;15:120-31.